Available online at www.sciencedirect.com
SCIENCE DIRECT
Journal of Solid State Chemistry 179 (2006) 2571–2577
JOURNAL OF SOLID STATE CHEMISTRY
www.elsevier.com/locate/jssc

Synthesis, structure and luminescence property of two lanthanum phosphite hydrates: $La_2(H_2O)_x(HPO_3)_3$ ($x = 1, 2$)

Ding-Bang Xiong[a,b], Man-Rong Li[a], Wei Liu[a], Hao-Hong Chen[a], Xin-Xin Yang[a], Jing-Tai Zhao[a,*]

[a]*The State Key Laboratory of High Performance Ceramics and Superfine Microstructure, Shanghai Institute of Ceramics, Chinese Academy of Science, Shanghai 200050, China*
[b]*Graduate School of Chinese Academy of Science, Beijing, P.R. China*

Received 6 March 2006; received in revised form 24 April 2006; accepted 27 April 2006
Available online 13 May 2006

Abstract

Two new lanthanum phosphite hydrates, $La_2(H_2O)(HPO_3)_3$ (**1**) and $La_2(H_2O)_2(HPO_3)_3$ (**2**), were synthesized by a hydrothermal method. Their crystal structures were determined by X-ray single-crystal method (**1**, monoclinic, $C2/c$ (No. 15); $a = 20.820(5)$ Å, $b = 6.717(2)$ Å, $c = 14.123(3)$ Å, $\beta = 101.261(3)^\circ$, $V = 1937.0(8)$ Å^3; $Z = 8$; **2**, triclinic, $P\text{-}1$ (No. 2); $a = 8.168(3)$Å, $b = 8.439(2)$ Å, $c = 9.337(3)$Å, $\alpha = 115.641(3)^\circ$, $\beta = 98.655(3)^\circ$, $\gamma = 105.124(3)^\circ$, $V = 533.87(1)$ Å^3, $Z = 2$). Both crystal structures present three-dimensional open-framework structures containing channels, and **1** adopts intersecting type. In the two structures, the face-sharing dimers of LaO_n ($n = 8, 9$) were observed. Other characterizations by IR and TG–DSC were also described. Furthermore, both the compounds doped with Ce^{+3} showed intensive broad emission band around 340 nm under UV excitation.
© 2006 Elsevier Inc. All rights reserved.

Keywords: Hydrothermal synthesis; Crystal structure; Lanthanum phosphite hydrate; Luminescence property

1. Introduction

Following the discovery of microporous crystalline aluminophosphates in 1980s [1,2], new open-framework metal phosphates have attracted considerable attention because of their potential applications in catalysis, adsorption, ionic conduction, ion exchange, electronics and optoelectronics. During the past decade, a large number of new metal phosphates with open frameworks have appeared in the literature. The metals include Ga [3], In [4,5], Zn [6,7], Fe ([8] and references therein), Sn ([9] and references therein), V [10–12], Mo [13], Ti [14], Mn [15] and rare-earth elements [16,17]. In the past few years, the pyramidal hydrogen phosphite ion $[HPO_3]^{2-}$ has also been incorporated into the structural framework of these kinds of compounds, giving rise to new purely inorganic [18] or organically templated phases [19]. In contrast to the large numbers of transition-metal phosphites, the reports on rare-earth phosphites are rare. According to the connectivity way of LnO_n polyhedra, we can sort them into two types of compounds containing chain and layer, respectively. In the type of chain, LnO_n polyhedra formed into a linear chain connected by their edges. Complexes of the lanthanide metals (La, Ce, Pr, Nd, Eu) [20–23] with phosphite and hypophosphite ligands were reported, such as $Eu_2(HPO_3)_3(H_2O)_{2.5}$, $La(HO_3PH)(HPO_3)\cdot 3H_2O$ and $\{Pr(H_2PO_2)(HPO_3)H_2O\}H_2O$. In the compounds (Pr, Nd, Eu) [24,25] containing layers, the framework almost was built from linear chains connected through corners or edges, such as $Ln_2(HPO_3)_3(H_2O)$(Ln = Pr, Nd) and $Eu_2(HPO_3)_3$. In all the compounds, no face-sharing polyhedra were observed.

Recently, we have synthesized some transition-metal phosphites, $(C_2H_{10}N_2)[Zn(HPO_3)_2]$ and $Na_2[M(HPO_3)_2]$ (M = Fe, Co) [26], with new structure types and relative properties have also been studied. In this work, our study was extended to the hydrothermal synthesis and crystal

*Corresponding author. Fax: +0086 021 5241312.
E-mail address: jtzhao@mail.sic.ac.cn (J.-T. Zhao).

0022-4596/$ - see front matter © 2006 Elsevier Inc. All rights reserved.
doi:10.1016/j.jssc.2006.04.035

structure determination of two new lanthanum phosphite monohydrate $La_2(H_2O)(HPO_3)_3$ (**1**) and lanthanum phosphite dihydrate $La_2(H_2O)_2(HPO_3)_3$ (**2**), which have an open three-dimensional (3D) framework containing face-sharing dimers and channels. In addition, the luminescence properties of both the compounds doped with Ce^{+3} were investigated.

2. Experimental section

2.1. Synthesis

All commercially available reagents and chemicals were of analytical or reagent-grade purity and used as received. Compounds **1** and **2** were prepared under mild hydrothermal conditions. Lanthanum chloride solution was prepared by adding the excess quantity of concentrated HCl (35% solution) to a suspension of the lanthanum oxide in water.

In the case of **1**, solution of $LaCl_3$ was used as the starting material. The solid of H_3PO_3 (0.410 g) was added to the solution of the lanthanum chloride (1 M, 10 mL) under constant stirring. Then the mixture was transferred into Teflon-lined stainless steel autoclave and heated for 5 days at 413 K under autogenous pressure. Colorless products were obtained by filtration and washed with water and dried in air at 333 K. For the case of **2**, the product was also obtained under the same hydrothermal conditions from a mixture of $LaCl_3$ solution (1 M, 10 mL), H_3PO_3(0.410 g), but $NH_4HB_4O_7 \cdot 3H_2O$(1.000 g) was added as additive agent.

2.2. Crystal structure determination

Crystals from each product were selected under a polarizing microscope, glued to a thin glass fiber with cyanoacrylate (superglue) adhesive, and inspected for singularity. Two of them were chosen ($0.05 \times 0.05 \times 0.10\,mm^3$ for **1** and $0.04 \times 0.04 \times 0.05\,mm^3$ for **2**), and data sets were collected on a Nonius Kappa CCD diffractometer (Mo$K\alpha$ radiation, 0.710 73 Å). The data were corrected for absorption using the SADABS program. The structures were solved by direct methods and refined against $|F^2|$ with the aid of the SHELXTL-PLUS package [27]. All hydrogen positions were located from the difference Fourier map but were refined as riding in the final refinement. Additional information about the data collection and structure refinement is presented in Table 1, while selected distances for **1** and **2** are listed in Tables 2 and 3, respectively.

2.3. Other characterizations

The products used for spectral measurements were also examined by powder X-ray diffraction (Rigaku D/max 2550 V diffractometer, Cu$K\alpha$) to confirm their phase identity and purity. The diffraction patterns were consistent with those calculated from the structures determined by single-crystal X-ray diffraction. IR spectra were collected on a Digilab-FTS-80 spectrophotometer using pressed KBr pellets of the samples. Thermogravimetric analysis was performed on an STA-409PC/4/H LUXX DSC-TGA instrument at a heating rate of $10\,K\,min^{-1}$ in a flow of N_2 to a maximum temperature of 1173 K. UV

Table 1
Data collection and processing parameters for $La_2(H_2O)(HPO_3)_3$and $La_2(H_2O)_2(HPO_3)_3$

Struct. param.	**1**	**2**
Empirical formula	$La_2(H_2O)(HPO_3)_3$	$La_2(H_2O)_2(HPO_3)_3$
Formula weight	535.77	553.79
Wavelength	0.71073 Å	0.71073 Å
Crystal system, space group	Monoclinic *C2/c* (No. 15)	Triclinic *P*-1 (No. 2)
Unit cell dimensions	$a = 20.820(5)$ Å,	$a = 8.168(2)$ Å, $\alpha = 115.641(3)^\circ$
	$b = 6.717(6)$ Å, $\beta = 101.261(3)^\circ$	$b = 8.439(2)$ Å, $\beta = 98.655(3)^\circ$
	$c = 14.123(3)$ Å,	$c = 9.337(2$ Å, $\gamma = 105.124(3)^\circ$
Volume	1937.0(8) Å^3	533.9(2) Å^3
Z, Calculated density (g/cm^3)	8, 3.674	2, 3.45
Absorption coefficient (mm^{-1})	9.234	8.388
$F(000)$	1952	508
θ range for data collection	1.99–27.10°	2.54–27.08°
Limiting indices	$24<=h<=26$, $-6<=k<=8$, $-17<=l<=17$	$-9<=h<=10$, $-10<=k<=9$, $-11<=l<=11$
Reflections collected/unique	4532/2096 [R(int) = 0.0167]	2674/2258 [R(int) = 0.0191]
Goodness-of-fit on F2	1.176	1.111
Final R indices [$I>2\sigma$(I)]	$R1 = 0.0231$[a], w$R_2 = 0.0554$[b]	$R1 = 0.0350$[a], w$R_2 = 0.0798$[b]
R indices (all data)	$R1 = 0.0246$, w$R_2 = 0.0561$	$R1 = 0.0403$, w$R_2 = 0.0826$
Largest diff. peak and hole	1.092 and −0.854 e Å^3	1.486 and −1.229 e Å^3

[a] $R_1 = \sum||F_0|-|F_0||/\sum|F_0|$.
[b] $wR_2 = \{\sum[w(F_0^2-F_0^2)^2]/\sum[w(F_0^2)^2]\}^{1/2}$.

Table 2
Selected bond lengths (Å) for $La_2(H_2O)(HPO_3)_3$

La(1)–O(7)$^{\#1}$	2.422(4)	La(1)–O(8)	2.450(3)
La(1)–O(1)$^{\#2}$	2.467(3)	La(1)–O(5)$^{\#3}$	2.533(3)
La(1)–O(2)$^{\#4}$	2.537(3)	La(1)–O(3)$^{\#3}$	2.547(3)
La(1)–O(10)	2.577(4)	La(1)–O(9)	2.847(3)
La(2)–O(6)$^{\#5}$	2.483(3)	La(2)–O(6)	2.515(3)
La(2)–O(9)	2.528(3)	La(2)–O(8)	2.551(3)
La(2)–O(4)$^{\#5}$	2.565(3)	La(2)–O(4)$^{\#6}$	2.585(3)
La(2)–O(5)$^{\#3}$	2.611(3)	La(2)–O(2)	2.648(3)
La(2)–O(1)	2.675(3)		
P(1)–O(3)	1.502(3)	P(1)–O(2)	1.530(3)
P(1)–O(6)	1.532(3)	P(1)–H(1)	1.507
P(2)–O(5)	1.529(3)	P(2)–O(4)	1.547(3)
P(2)–O(9)	1.519(3)	P(1)–H(2)	1.298
P(3)–O(7)	1.498(4)	P(3)–O(1)	1.527(3)
P(3)–O(8)	1.533(3)	P(1)–H(3)	1.425

Symmetry transformations used to generate equivalent atoms: #1, $-x+1$, y, $-z+3/2$; #2, x, $-y$, $z+1/2$; #3, $-x+1/2$, $y-1/2$, $-z+3/2$; #4, $-x+1/2$, $y+1/2$, $-z+3/2$; #5, $-x+1/2$, $-y+1/2$, $-z+1$; #6, x, $y-1$, z; #7, x, $-y$, $z-1/2$; #8, x, $y+1$, z.

Table 3
Selected bond lengths (Å) for $La_2(H_2O)_2(HPO_3)_3$

La(1)–O(5)	2.451(5)	La(1)–O(4)$^{\#1}$	2.459(5)
La(1)–O(1)$^{\#2}$	2.462(5)	La(1)–O(8)$^{\#3}$	2.480(5)
La(1)–O(2)$^{\#3}$	2.585(5)	La(1)–O(11)	2.619(5)
La(1)–O(7)	2.661(5)	La(1)–O(4)	2.673(5)
La(1)–O(6)$^{\#3}$	2.812(5)		
La(2)–O(9)$^{\#4}$	2.416(5)	La(2)–O(3)$^{\#5}$	2.461(5)
La(2)–O(7)	2.512(5)	La(2)–O(6)$^{\#3}$	2.554(5)
La(2)–O(2)	2.568(5)	La(2)–O(3)	2.589(5)
La(2)–O(10)	2.632(6)	La(2)–O(5)	2.705(5)
La(2)–O(8)	2.878(5)		
P(1)–O(5)	1.505(5)	P(1)–O(6)	1.518(5)
P(1)–O(2)	1.541(5)	P(1)–H(1)	1.306
P(2)–O(1)	1.514(5)	P(2)–O(8)	1.517(5)
P(2)–O(3)	1.544(5)	P(2)–H(3)	1.374
P(3)–O(9)	1.502(5)	P(3)–O(4)	1.533(5)
P(3)–O(7)	1.537(5)	P(3)–H(2)	1.362

Symmetry transformations used to generate equivalent atoms: #1, $-x$, $-y$, $-z+2$; #2, $x-1$, y, z; #3, $-x+1$, $-y+1$, $-z+2$; #4, $-x$, $-y$, $-z+1$; #5, $-x+1$, $-y$, $-z+1$; #6, $x+1$, y, z.

luminescence spectra were recorded on a Shimadyn RF-5301 spectrofluorophotometer at room temperature and a 450 W xenon lamp was used as an excitation source.

3. Result and discussion

3.1. Synthesis

Compound **1** was obtained through the reaction of H_3PO_3 with the solution of $LaCl_3$ directly under mild hydrothermal conditions. Compound **2** was obtained under the same condition, except that $NH_4HB_4O_7 \cdot 3H_2O$ was added as additive agent. The precursors were stirred for 2 h and the acidity of both precursors reached pH = 1.0 at last. According to the experiment, we can note that $NH_4HB_4O_7 \cdot 3H_2O$ did not influence the pH value of the later solution. So the addition of $NH_4HB_4O_7 \cdot 3H_2O$ played an important role in producing the difference. To investigate the influence of $NH_4HB_4O_7 \cdot 3H_2O$ on the reaction, we replaced it by NH_4Cl and $Na_2B_4O_7 \cdot 10H_2O$, but we did not obtain compound **2** in both cases. Therefore, $NH_4HB_4O_7 \cdot 3H_2O$ acted as a sort of catalyst in the reaction, and the mechanism is under investigation.

3.2. Structure description

3.2.1. $La_2(H_2O)(HPO_3)_3$

Selected bond distances are given in Table 2. There are two types of lanthanum groups and three types of phosphite groups in terms of their mode of coordination. The one containing La1 atom is an eight-coordinated bicapped trigonal prism, while the other containing La2 is a nine-coordinated tricapped trigonal prism as shown in Fig. 1a. In LaO_8 polyhedra, seven of the oxygen atoms bonded to La originate from phosphite groups, while the eighth is from a coordinated water molecule (O10). In LaO9 polyhedra, coordinated oxygen atoms originate from seven phosphite groups, with each La2 surrounded by two bidentate phosphite anions and five monodentate phosphite anions. An LaO_8 and an LaO_9 share a face bridged by O5, O8 and O9 forming a dimer. The face-sharing polyhedral dimers La(1)O_8–La(2)O_9 are the secondary

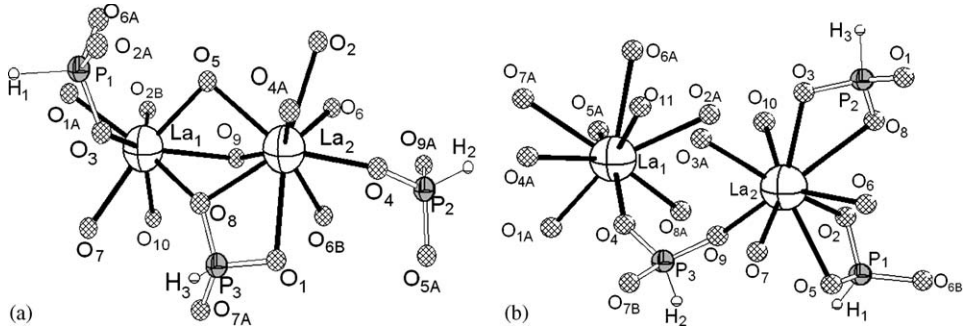

Fig. 1. ORTEP of the asymmetric unit of $La_2(H_2O)(HPO_3)_3$(a) and $La_2(H_2O)_2(HPO_3)_3$(b)showing 50% probability ellipsoids and the labeling scheme. Only the hydrogen associated with the phosphorus are shown.

building block (SBU), and they form zigzag chains by sharing edges. These chains are connected to each other by sharing corners and also linked by phosphite units leading to layers parallel to the (100) plane (Fig. 2a). Then these layers further form 3D open-framework by sharing corners with the phosphite tetrahedra in adjacent layers (Fig. 2b), and their linkage strengthened by hydrogen bonds (O10–H4⋯O10 = 2.344 Å, O10–H4⋯O10 = 1.874 Å) (Fig. 3a) through the coordinated water. This gives rise to the formation of four-ring channels (size in 4.808 × 3.574 Å) along [010] crossing with star-like four-ring channels (size in 5.757 × 2.047 Å) along [001]. From Fig. 3a, we can see that there are two types of four-ring channels along [010] with one of them occupied by the coordinated water molecules and the other is hollow, and they are arranged alternately along *c*-axis.

3.2.2. $La_2(H_2O)_2(HPO_3)_3$

Selected bond distances are given in Table 3. There are two crystallographically distinct La atoms and three P atoms as can be seen in Fig. 1b. The La atoms are nine-coordinated (both adopt tricapped triangular prism type) by the oxygen atoms from two bidentate phosphite, four monodentate phosphite and one water molecule (O11). Two crystallographically distinct LaO_9 share a face bridged by O5, O6 and O7 forming a dimer. In this structure, the face-sharing polyhedral dimer La(1)O_9–La(2)O_9 is also characteristic as SBU. Dimers share their edges and form a layer including four-membered and eight-membered rings parallel to (1–11). In the layer, two stagger phosphite tetrahedra cap the four-membered ring on either side. The eight-membered ring is incompletely filled by four phosphite tetrahedral (Fig. 4a). Then these layers are connected only by phosphite polyhedra forming 3D framework (Fig. 4b), which strengthened via hydrogen bonds (O10–H5⋯O9 = 2.244 Å, O10–H4⋯O3(andO8) = 2.083(1.925)Å, O11–H6⋯O2=2.106 Å, O11–H4⋯O10=2.072 Å) (Fig. 3b). In the hydrogen bond O10–H4⋯O, there are two alternative approximate oxygen atom positions, O3 and O8, for H4, and form two different strength bonds. This gives rise to the formation of six-ring channels (size in 8.087 × 3.608 Å) along [100], and two coordinated water molecules are located in the channels (Fig. 3b).

The face-sharing connectivity of LaO_n ($n = 8, 9$) polyhedra in the framework of compounds **1** and **2** is unique while comparing other known phosphates [20–25]. In the known phosphites, LaO_n polyhedra present linear chains in most cases ($La(H_2PO_3)_3(HPO_3)(H_2O)_3$ in Fig. 5a), except

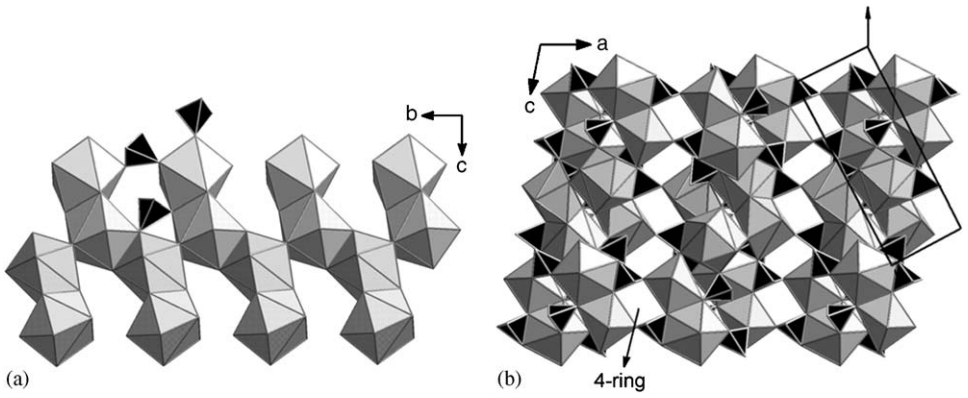

Fig. 2. The dissection and arrangement of the structure of $La_2(H_2O)(HPO_3)_3$. (a) The edge-connected zigzag chain of face-sharing La-centered polyhedra dimer, and the location of the chain in the structure is shown by the rectangle in (b). The manner of the connectivity of La-centered polyhedra and phosphite polyhedra was indicated by the selected phosphite; (b) The overview of open-framework structure of the compound. The direction of projection is indicated in figure. Only three phosphite groups were shown here for clarity. For further details see text.

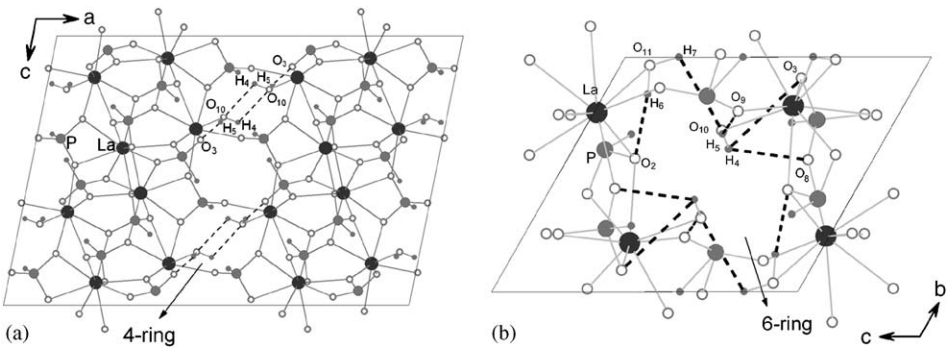

Fig. 3. The stick connectivity of $La_2(H_2O)(HPO_3)_3$ in which 4-ring could be seen (a) and $La_2(H_2O)_2(HPO_3)_3$, in which a 6-ring could be seen (b). Dashed lines indicate probable hydrogen bond.

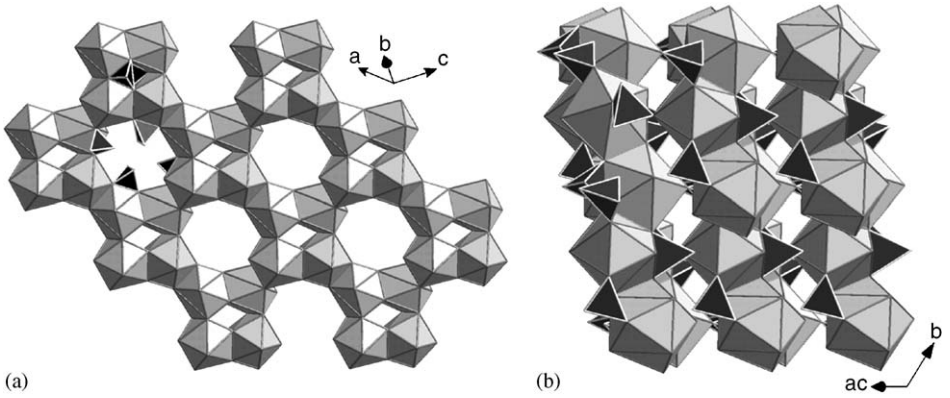

Fig. 4. The dissection and package of the structure of $La_2(H_2O)_2(HPO_3)_3$. (a) The edge-sharing connectivity of face-sharing La-centered polyhedra dimer, and form a polyhedra layer containing 4-membered ring and 8-membered ring. The manner of the connectivity of La-centered polyhedra and phosphite polyhedra was indicated by the selected phosphite; (b) The overview of open-framework structure of the compound. The direction of projection is indicated in figure. Only three pairs of phosphite were shown here for clarity. For further details see text.

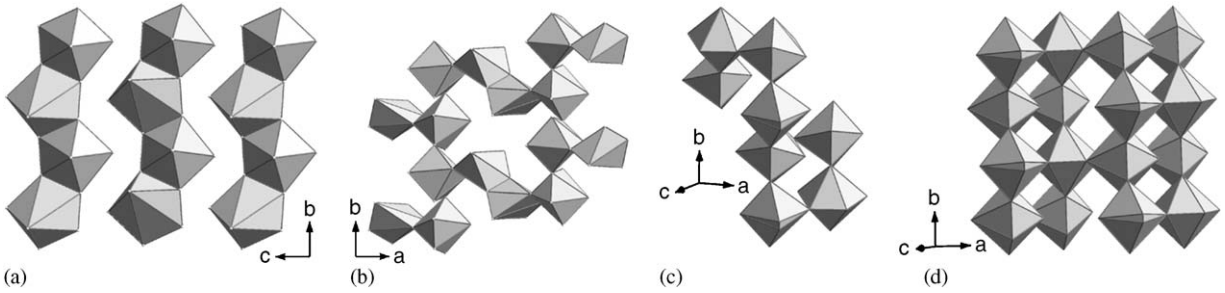

Fig. 5. The different way of connectivity between LaO_n polyhedra in other known phosphites: (a) linear chain in $La(H_2PO_3)_3(HPO_3)(H_2O)_3$; (b)layer comprises chains connected by edge-sharing dipolyhedra through edge in $Ln_2(HPO_3)_3(H_2O)$(Ln = Pr, Nd); (c) and (d)layer comprises chains connected through edge and corner alternately in $Eu_2(HPO_3)_3$.

that some other adopt layer structures ($Ln_2(HPO_3)_3(H_2O)$ (Ln = Pr, Nd) and $Eu_2(HPO_3)_3$ in Fig. 5b–d). The chain in compound **1** (Fig. 2a) and layer in compound **2** (Fig. 4a) present some new structural features in rare-earth phosphites. The La–La distances of 3.986 and 4.045 Å in the dimer in compounds **1** and **2** are the shortest ones in known phosphites, e.g., 9.826 Å in $La(H_2PO_3)_3(HPO_3)(H_2O)_3$ [20] and 4.016 Å in $Eu_2(HPO_3)_3$ (Fig. 6). [25] It is interesting to note that such short distances may lead to some attractive properties when extended to other rare-earth systems and the investigation is on the way.

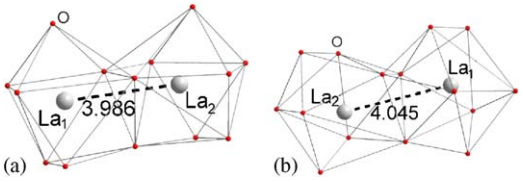

Fig. 6. A view of the dimer formed by face-sharing coordination polyhedra in the compound (a) $La_2(H_2O)(HPO_3)_3$ and (b) $La_2(H_2O)_2(HPO_3)_3$. The dotted line show the distance between La in the dimer.

The infrared spectrum of compounds exhibits strong and sharp peak at υ(HP), 2495, 2399, 2345 cm^{-1}; δ(HP), 1030 cm^{-1} and υ(HP), 2468, 2379, 2426 cm^{-1}; δ(HP), 1034 cm^{-1}, indicative of P–H linkages in structures **1** and **2**, respectively, providing additional evidence for the phosphite structure [19d]. A number of symmetric and antisymmetric P–O stretching modes are observed in 1200–950 cm^{-1}, and symmetric and antisymmetric P–O deformation modes in 580–450 cm^{-1} range. The "free" H_2O group has three modes of internal vibration occurring at frequencies 3765, 3652 and 1640 cm^{-1} [28]. In our result, all modes of internal vibration of H_2O shift to lower frequencies from their ideal value because of hydrogen bonding. Hydrogen bonding manifests itself in the strong and broad features at ca. 3600–2700 cm^{-1}, and the band is broader but weaker in the spectrum of **1** than in that of **2**, with a decoupling of bands at 1658 and 1627 cm^{-1} in **2,** indicating at least two types of water molecules different from that in compound **1** [29]. The internal vibration of crystal water molecules in **1** is a single peak at around 1630 cm^{-1}.

Thermogravimetic analysis indicated the weight loss of sample **1** ca. 3.45% in the temperature range from 300 to 400 °C in one step, corresponding to the lost of one water molecule (calcd. 3.36%). Similarly, the weight loss of sample **2** ca. 6.22% in the temperature range from 200 to

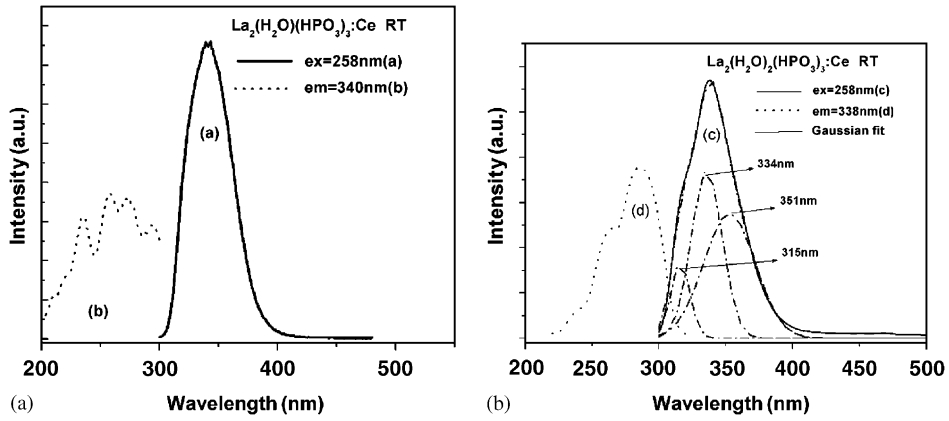

Fig. 7. UV excited (ex = 258 nm) emission spectrum(a) and excitation (em = 340 nm) spectrum (b) of phosphor $La_2(H_2O)(HPO_3)_3:Ce^{3+}$, and UV excited (ex = 258 nm) emission spectrum (c) and excitation (em = 358 nm) spectrum (d) of phosphor $La_2(H_2O)_2(HPO_3)_3:Ce^{3+}$ at 293 K.

350 °C in one step, corresponding to the loss of two water molecules (calcd. 6.41%). From the X-ray diffraction results, both the samples transferred into un-identified phases after TG analysis.

4. Photoluminescence spectroscopy

Investigations on the luminescent properties of these two compounds doped with Ce^{+3} under UV excitation have been performed. The emission and excitation spectra of $La_2(H_2O)(HPO_3)_3:Ce^{3+}$ and $La_2(H_2O)_2(HPO_3)_3:Ce^{3+}$ at room temperature are presented in Fig. 7. By monitoring the emission at 340 nm, the *f–d* excitation band of Ce^{3+} can be observed with peaks at 236, 258, 273 and 294 nm in $La_2(H_2O)(HPO_3)_3:Ce^{3+}$, and 240, 264 and 285 nm in $La_2(H_2O)_2(HPO_3)_3:Ce^{3+}$.The emission spectrums for $La_2(H_2O)(HPO_3)_3:Ce^{3+}$ show one broadband around 339 nm, while for $La_2(H_2O)_2(HPO_3)_3:Ce^{3+}$, the broadband around 340 nm must be divided into three peaks at about 315, 334 and 351 nm by Gaussian multi-peak fits. These emission peaks can be attributed to the $5d–2F_{5/2}$ and $5d–2F_{7/2}$ transition of Ce^{3+} occupied different sites, but the exact mechanism caused the different emission peaks between the two compounds is not yet understood. We also optimize the doping concentration and get the conclusion that the intensity reached maximum when the concentration is around 1.8 mol% in both compounds.

5. Conclusion

Two lanthanum phosphates, **1** and **2**, were synthesized by mild hydrothermal reaction. For **1** and **2**, the 3D open-framework structures are built up from dimers of face-sharing of La-centered polyhedra and phosphite groups with different arrangements. For compound **1**, dimers form unique zigzag chains shared by edges, and then these chains are connected into 3D framework by phosphite group through corners and also between dimers. The framework adopts intersecting channels along [010) and [001], respectively. For compound **2**, dimers form unique layer shared by edges containing four and eight rings; then layers are connected into 3D framework by phosphite group through corners. The framework contains six-ring channels along [100]. For emission spectrum of the two Ce^{+3}-doped compounds, both have a broadband around 340 nm.

Acknowledgment

This work was supported by the Key Project (50332050) from the NNSF of China and from the Hundred Talents Program from the Chinese Academy of Sciences and fund for Young Leading Researchers from Shanghai municipal government. The authors thank Ying-Jie Zhu's research group for their great help in measuring TG–DSC. Helpful discussions with Professor Huang Fu-Qiang are also greatly acknowledged.

Appendix A. Supplementary materials

Supplementary data associated with this article can be found in the online version at doi:10.1016/j.jssc.2006.04.035.

References

[1] S.T. Wilson, B.M. Lok, C.A. Messina, T.R. Cannan, E.M. Flanigen, J. Am. Chem. Soc. 104 (1982) 1146.
[2] M.E. Davis, C. Saldarriage, C. Montes, J. Garces, C. Crowder, Nature 331 (1988) 698.
[3] R. Xu, J. Chen, S. Feng, Stud. Surf. Sci. Catal. 60 (1991) 63.
[4] I.D. Williams, J. Yu, H. Du, J. Chen, W. Pang, Chem. Mater. 10 (1998) 773.
[5] S.S. Dhingra, R.C. Haushalter, J. Chem. Soc., Chem. Commun. (1993) 1665.
[6] W.T.A. Harrison, T.E. Martin, T.E. Gier, G.D. Stucky, J. Mater. Chem. 2 (1992) 175.
[7] G. Yang, S.C. Sevov, J. Am. Chem. Soc. 121 (1999) 8389.
[8] K.-H. Lii, Y.-F. Huang, V. Zima, C.-Y. Huang, H.-M. Lin, Y.-C. Jiang, F.-L. Liao, S.-L. Wang, S. Wang, Chem. Mater. 10 (1998) 2599.

[9] S. Natarajan, S. Ayyappan, A.K. Cheetham, C.N.R. Rao, Chem. Mater. 10 (1998) 1627.
[10] Y. Zhang, A. Clearfield, R.C. Haushalter, Chem. Mater. 7 (1995) 1221.
[11] Z. Bircask, W.T.A. Harrison, Inorg. Chem. 37 (1998) 3204.
[12] M.I. Khan, L.M. Meyer, R.C. Haushalter, A.L. Schweizter, J. Zubieta, J.L. Dye, Chem. Mater. 8 (1996) 43.
[13] R.C. Haushalter, L.A. Mundi, Chem. Mater. 4 (1992) 31.
[14] Y. Liu, Zh. Shi, L. Zhang, Y. Fu, J. Chen, B. Li, J. Hua, W. Pang, Chem. Mater. 13 (2001) 2017.
[15] (a) J. Escobal, J.L. Pizarro, J.L. Mesa, L. Lezama, R. Olazcuaga, M.I. Arriortua, T. Rojo, Chem. Mater. 12 (2000) 376;
(b) Y. Song, P.Y. Zavalij, N.A. Chernova, M.S. Whittingham, Chem. Mater. 15 (2003) 4968.
[16] S.B.I. Moussa, J.E. Sobrados, M. Iglesias, Trabelsi-Ayedi, J. Sanz, J. Mater. Chem. 10 (2000) 1973.
[17] S.B. Moussa, S. Ventemillas, A. Cabeza, E. Gutierrez-Puebla, J. Sanza, J. Solid State Chem. 177 (2004) 2129.
[18] (a) R.E. Morris, W.T.A. Harrison, J.M. Nicol, A.P. Wikinson, A.K. Cheetham, Nature 359 (1992) 519;
(b) S. Minghuey, J.M. Kevin, J.S. Philip, C. Abraham, Inorg. Chem. 29 (1990) 959;
(c) M.D. Marcos, P. Amoros, A. Beltran, R. Martinez, J.P. Attfields, Chem. Mater. 5 (1993) 121;
(d) M.D. Marcos, P. Amoros, A.L. Bail, J. Solid State Chem. 107 (1993) 250;
(e) J. Ensling, J.P. Gutlich, R. Schmidt, R. Kniep, Inorg. Chem. 33 (1994) 3595;
(f) C.Y. Ortiz-Avila, P.J. Squattrito, M. Shieh, A. Clearfield, Inorg. Chem. 28 (1989) 2608.
[19] (a) S. Fernandez, J.L. Mesa, J. Pizarro, J.S. Garitaonandia, M.I. Arriortua, T. Rojo, Angew. Chem. Int. Ed. 43 (2004) 977;
(b) M.L.F. Phillips, T.M. Nenoff, C.T. Thompson, W.T.A. Harrison, J. Solid State Chem. 167 (2002) 337;
(c) S. Fernandez, J.L. Mesa, J. Pizarro, L. Lezama, M.I. Arriortua, T. Rojo, Chem. Mater. 14 (2002) 2300;
(d) S. Fernandez, J. Mesa, J. Pizarro, L. Lezama, M.I. Arriortua, T. Rojo, Chem. Mater. 15 (2003) 1204;
(e) Y. Wang, J.H. Yu, Y. Du, Zh. Shi, Y.C. Zou, R.R. Xu, J. Chem. Soc., Dalton Trans. (2002) 4060;
(f) S. Mandal, S.K. Pati, M.A. Green, S. Natarajan, Chem. Mater. 17 (2005) 638.
[20] Y. Zhang, H. Hu, A. Clearfield, Inorg. Chim. Acta. 193 (1992) 35.
[21] J.A. Seddon, A.R.W. Jackson, R.A. Kresinski, A.W.G. Platt, J. Chem. Soc., Dalton Trans. (1999) 2189.
[22] (a) M. Loukili, J. Durand, L. Cot, M. Rafiq, Acta Crystallogr. C 44 (1988) 6;
(b) M. Loukili, J. Durand, A. Larbot, L. Cot, M. Rafiq, Acta Crystallogr. C 47 (1991) 477;
(c) N. Tijani, J. Durand, L. Cot, Acta Crystallogr. C 44 (1988) 2048.
[23] J.-D. Foulon, N. Tijani, J. Durand, M. Rafiq, L. Cot, Acta Crystallogr. C 49 (1993) 849.
[24] J.-D. Foulon, N. Tijani, J. Durand, M. Rafiq, L. Cot, Acta Crystallogr. C 49 (1993) 1.
[25] J.-D. Foulon, J. Durand, L. Cot, N. Tijani, M. Rafiq, Acta Crystallogr. C 51 (1995) 348.
[26] (a) W. Liu, H.H. Chen, X.X. Yang, J.T. Zhao, J. Alloys Compounds 392 (2005) 100;
(b) W. Liu, H.H. Chen, X.X. Yang, J.T. Zhao, Eur. J. Inorg. Chem. (2005) 946.
[27] G.M. Sheldrick, SHELXTL Programs, Release Version 5.1, Bruker AXS, Madison, WI, 1998.
[28] H.D. Lutz, Struct. Bonding 69 (1988) 7.
[29] L. Herschke, V. Enkelmann, I. Lieberwirth, G. Wegner, Chem. Eur. J. 10 (2004) 2795.